

## Unstable topography of biphasic surfactant monolayers

H. DIAMANT<sup>1</sup>(\*), T. A. WITTEN<sup>1,2</sup>, A. GOPAL<sup>3</sup> and K. Y. C. LEE<sup>3</sup>

<sup>1</sup> *The James Franck Institute, The University of Chicago - Chicago, IL 60637, USA*

<sup>2</sup> *Department of Physics, The University of Chicago - Chicago, IL 60637, USA*

<sup>3</sup> *Department of Chemistry and Institute for Biophysical Dynamics  
The University of Chicago, Chicago, IL 60637, USA*

(received 25 May 2000; accepted in final form 4 September 2000)

PACS. 68.10.Et – Interface elasticity, viscosity, and viscoelasticity.

PACS. 87.68.+z – Biomaterials and biological interfaces.

PACS. 82.70.Kj – Emulsions and suspensions.

**Abstract.** – We study the conformation of a heterogeneous surfactant monolayer at a fluid-fluid interface, near a boundary between two lateral regions of differing elastic properties. The monolayer attains a conformation of shallow, steep “mesas” with a height difference of up to 10 nm. If the monolayer is progressively compressed (*e.g.*, in a Langmuir trough), the profile develops overhangs and finally becomes unstable at a surface tension of about  $K(\delta c_0)^2$ , where  $\delta c_0$  is the difference in spontaneous curvature and  $K$  a bending stiffness. We discuss the relevance of this instability to recently observed folding behavior in lung surfactant monolayers, and to the absence of domain structures in films separating oil and water in emulsions.

Insoluble (Langmuir) monolayers of amphiphilic molecules, lying at water-air or water-oil interfaces, have been extensively studied in the past decades [1]. Such monolayers are found in many applications, including, *e.g.*, surface-tension reduction, emulsification and coating. Of particular interest are phospholipid monolayers, which are used in various studies to model the surface of cell membranes [2]. Lipid monolayers are encountered in other biological systems, such as the lung surfactant monolayer coating the alveoli in lungs [3].

An interesting issue is the departure of a monolayer, upon lateral compression, from a flat, two-dimensional conformation to a buckled, three-dimensional one. This aspect is particularly important in the case of lung surfactant monolayers, which undergo compression/expansion cycles during breathing. The buckling transition was theoretically studied in previous works [4–6]. These studies focused on the overall conformation of the entire monolayer, seeking an instability with respect to a single extended mode (or a prescribed combination of modes [6]) of undulation. They yield a buckling transition at a practically vanishing surface tension (*i.e.*, very high compression).

In many circumstances the monolayer is inhomogeneous. The heterogeneity may arise in single-component monolayers from the coexistence of expanded and condensed domains [7]; multi-component monolayers may phase-separate to form domains of different composition. The coupling between conformation and inhomogeneous composition was thoroughly studied as well [6, 8–13], usually focusing on bilayer membranes. These works considered annealed

---

(\*) E-mail: [diamant@control.uchicago.edu](mailto:diamant@control.uchicago.edu)

variations in composition, leading to spontaneous formation of ripples, modulated phases and shape transformations.

Unlike symmetric bilayers, lipid monolayers usually have a finite spontaneous curvature, arising either from the asymmetry of the lipid molecule itself, or from electrostatic interactions (*i.e.*, the dielectric asymmetry between the aqueous and the non-polar air or oil phases) [14]. The common picture is that below the buckling transition the monolayer conformation is flat despite the spontaneous curvature. The reason is that the bending energy per unit area to be gained by a curved conformation (typically a few tenths of  $k_B T$  per  $\text{nm}^2$ ,  $k_B T$  being the thermal energy) is much smaller than the required work against surface tension (usually more than  $10 k_B T$  per  $\text{nm}^2$ ). Hence, only at very low tension (*i.e.*, high compression) is the monolayer expected to depart from a flat conformation and buckle. This argument, however, applies to the overall spatial behavior of a homogeneous monolayer.

In the current work we ask a different question: what is the *local* response of a Langmuir monolayer to a fixed profile in mechanical properties as arising from a lateral domain structure. There are four important length scales in the system: the typical domain size,  $L$ , the thickness of a domain boundary,  $d$ , the spontaneous radius of curvature,  $c_0^{-1}$ , and the elastic length,  $\lambda = (K/\gamma)^{1/2}$  determining the lateral length scale of height variations ( $K$  being the bending rigidity and  $\gamma$  the surface tension). The discussion in this letter is much simplified by assuming  $L \gg \lambda \gg d$  (the value of  $c_0$  remains unrestricted). Since  $L$  is of order  $10 \mu\text{m}$  and  $\lambda$  is typically  $1\text{--}10 \text{ nm}$ , the first inequality is well justified. It allows us to isolate a single, straight boundary, separating two infinite domains. The second assumption,  $\lambda \gg d$ , allows us to treat the domain boundary as infinitely sharp. In practice, for a biphasic layer far from its critical point,  $d$  is typically the size of a few headgroups, roughly  $1 \text{ nm}$  (though it may exceed the scale of  $\lambda$  in some circumstances). For typical  $d$  we find that the infinitely sharp limit is a good approximation [15]. An additional requirement is that the monolayer surface maintain its integrity throughout the compression. This is generally not the case in practice; lipid monolayers often fracture and form multi-layers at a finite pressure [16]. This occurs as the monolayer yields to vertical shear stresses, brought about by the lateral pressure combined with small curvature. Another mechanism encountered in practice is the ejection of vesicles into the aqueous phase [17]. However, the presence of certain additives in natural and model lung surfactants was found to suppress these microscopic types of collapse [18].

Using these observations, we can find the shape of the surface as a function of its projected area or surface tension, without the usual assumption of a moderate, single-valued height function. Thus, we implicitly take into account all modes of response and allow for overhangs. (A related calculation was previously presented for studying different domain shapes [19]. Being restricted to linear response, this model yielded mild height modulations in the form of stable “caplets”, rather than the sharp “mesas” and conformation instability found in the current work.)

We represent the boundary region of two large domains as a surface whose left and right halves differ in bending rigidity  $K$  and spontaneous curvature  $c_0$ . On the left half  $K = K_1$  and  $c_0 = c_{01}$ ; on the right half the values are  $K_2$  and  $c_{02}$ . The resulting surface is uniform in the direction parallel to the domain boundary but curved in the perpendicular direction, as shown in fig. 1b. We may thus represent the surface by its intersection with a vertical plane perpendicular to the boundary. We define the monolayer conformation by the local angle  $\theta(s)$  between the surface and a reference plane at curvilinear distance  $s$  from the domain boundary (see fig. 1b). The bending energy  $U$  of the monolayer can thus be written as  $U = L \int_{-\infty}^0 ds [\frac{1}{2} K_1 \dot{\theta}^2(s) - K_1 c_{01} \dot{\theta}(s)] + L \int_0^{\infty} ds [\frac{1}{2} K_2 \dot{\theta}^2(s) - K_2 c_{02} \dot{\theta}(s)]$ . Here  $L$  is the length of the domain boundary and  $\dot{\theta} \equiv d\theta/ds$  is the local curvature. We require that  $\theta(s)$  be

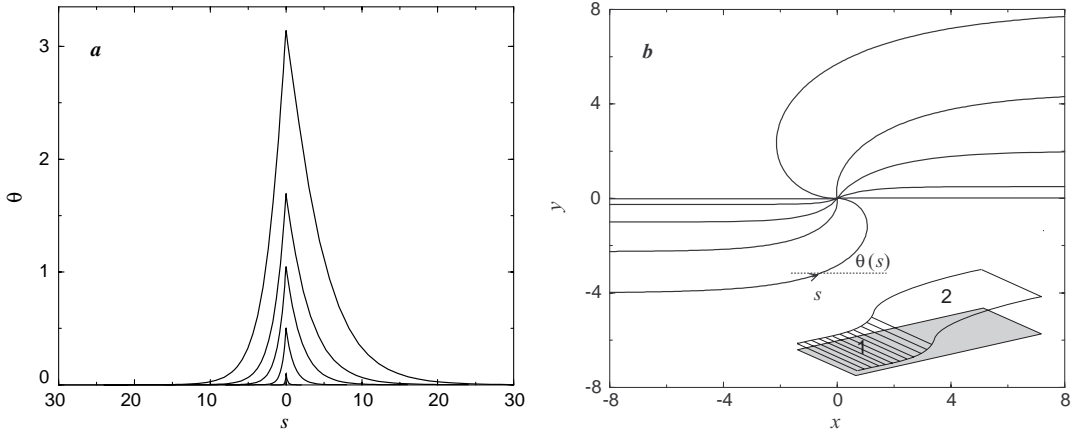


Fig. 1 – a) Slope angle profiles near a domain wall as compression is increased. The curves are obtained from eqs. (2)-(3) using the following parameters (from bottom to top):  $v = 0.1, 0.5, 1, 1.5, 2$ ;  $\lambda_1 = 0.1, 0.5, 1, 1.5, 2$ ;  $\lambda_2 = 0.2, 1, 2, 3, 4$ . (The proportions  $v:\lambda_1:\lambda_2$  are kept fixed so as to simulate a compression process, decreasing  $\gamma$  while keeping all other parameters constant.) b) The corresponding spatial conformations. The units of length are arbitrary (they are typically of order 10 nm). The inset shows a schematic three-dimensional sketch of the monolayer shape for  $\theta_0 < \pi/2$ .

continuous at  $s = 0$ , so that the surface is smooth everywhere. The state of minimum  $U$  (without including tension) is a curled surface with curvature  $c_{01}$  on the left and  $c_{02}$  on the right. Only a net tension  $\gamma$  in the monolayer allows the surface to approach a flat conformation. This tension adds a term  $-\gamma A_p$  to the energy, where  $A_p$  is the projected area of the surface, shown as a shaded plane in fig. 1b. The element of projected area is  $ds \cos \theta$ , so that the full energy to be minimized can be written as  $G \equiv U + \gamma L \int_{-\infty}^{\infty} ds [1 - \cos \theta(s)]$ .

Thus our system is equivalent to a pre-curved sheet of paper of length  $L$  joined at one edge to a more strongly curled sheet and then subjected to a tensile force  $\gamma L$  acting so as to straighten the curling. Even under large tensions, there is a non-zero departure from the flat state. To demonstrate this departure, we consider the bending moments of the two sheets across the junction line. The left side exerts a moment on the right side equal to  $\delta U / \delta \dot{\theta}(0^-) = LK_1[\dot{\theta}(0^-) - c_{01}]$ . This must equal the moment acting from the right side,  $LK_2[\dot{\theta}(0^+) - c_{02}]$ . Hence the curvatures on the two sides are in general unequal:  $K_1\dot{\theta}(0^-) - K_2\dot{\theta}(0^+) = K_1c_{01} - K_2c_{02} \equiv \Delta$ , where the parameter  $\Delta$  (having dimensions of force) characterizes the extent of heterogeneity. The non-zero curvature  $\dot{\theta}(0)$  at the boundary relaxes to zero on a distance  $\lambda$  (to be determined), producing a net slope angle  $\theta_0 \equiv \theta(s=0) \sim \lambda \dot{\theta}(0)$  with bending energy  $KL\lambda \dot{\theta}(0)^2$ . For small  $\theta_0$  the associated loss of projected area is of order  $L\lambda \theta_0^2$ , with energy  $\gamma L\lambda[\lambda \theta(0)]^2$ . The decay length  $\lambda$  is that which minimizes the total energy, *i.e.*,  $\lambda \sim (K/\gamma)^{1/2}$  as anticipated above. For  $K_1 = K_2$  the angle  $\theta_0$  is proportional to the difference in spontaneous curvature,  $\delta c_0 \equiv c_{01} - c_{02}$ :  $\theta_0 \sim (\Delta/K)\lambda \sim (K/\gamma)^{1/2} \delta c_0$ .

To show the explicit profile and the buckling instability, we rewrite the energy per unit length by integrating the linear term in  $\dot{\theta}$  while requiring that the monolayer be flat far away from the boundary (*i.e.*, at the centers of the two contiguous domains),  $\theta(s \rightarrow \pm\infty) = 0$ ,

$$g[\theta(s)] \equiv G/L = \int ds [(K/2)\dot{\theta}^2 + \gamma(1 - \cos \theta)] - \theta_0 \Delta. \quad (1)$$

Equation (1) has the familiar form of a physical pendulum action (with  $s$  as imaginary time).

Variation with respect to  $\theta(s \neq 0)$  gives the sine-Gordon equation,  $K_i \ddot{\theta} = \gamma \sin \theta$ ,  $i = 1, 2$ , whose first integration yields  $\dot{\theta}^2 = 4\lambda_i^{-2} \sin^2(\theta/2)$ . Second integration leads to soliton profiles on both sides of the boundary,

$$\tan(\theta/4) = \begin{cases} \tan(\theta_0/4)e^{s/\lambda_1}, & s < 0, \\ \tan(\theta_0/4)e^{-s/\lambda_2}, & s > 0. \end{cases} \quad (2)$$

Finally, the condition for the jump in curvature at the boundary (*e.g.*, as found above from a moment balance argument, or by variation of  $g$  with respect to  $\theta_0$ ) is  $K_1 \dot{\theta}(0^-) - K_2 \dot{\theta}(0^+) = \Delta$ , which determines  $\theta_0$  as

$$\sin(\theta_0/2) = \Delta/[2\sqrt{\gamma}(\sqrt{K_1} + \sqrt{K_2})] \equiv v/2. \quad (3)$$

Thus, for any finite  $\Delta$ , the monolayer has a sigmoidal shape whose maximum slope angle is given by  $\theta_0$  of eq. (3). The total height difference is given by

$$h = \int_{-\infty}^{\infty} ds \sin \theta = \Delta/\gamma. \quad (4)$$

Substituting the obtained profile back in eq. (1), we find the energy of the conformation,

$$g/\Delta = 2 \tan(\theta_0/4) - \theta_0 = 4(1 - \sqrt{1 - v^2/4})/v - 2 \sin^{-1}(v/2). \quad (5)$$

The relation between the projected area and surface tension is found by imposing the area constraint,  $A_p = L \int ds \cos \theta$ , or, equivalently, by taking the derivative of  $g$  with respect to  $\gamma$ ,

$$\delta L \equiv (A - A_p)/L = \partial g/\partial \gamma = [2(\sqrt{K_1} + \sqrt{K_2})^2/\Delta]v(1 - \sqrt{1 - v^2/4}). \quad (6)$$

According to eqs. (3)-(6), as compression is increased, *i.e.*,  $\delta L$  is increased or  $\gamma$  is decreased (depending on the experimental scenario), the step profile becomes sharper (larger  $\theta_0$ ), higher (larger  $h$ ), and more favorable (lower  $g$ ). The process is demonstrated in fig. 1. At a certain stage  $\theta_0$  becomes larger than  $\pi/2$  and an overhang forms. However, as is evident from eqs. (3)-(6), there is a critical value of compression beyond which the profile equations have no solution. Beyond this point our physical pendulum goes over the top and our model surface curls up. This happens when  $\theta_0$  reaches  $\pi$ , corresponding to  $v_c = 2$ , or

$$\gamma_c = [\Delta/2(\sqrt{K_1} + \sqrt{K_2})]^2 \simeq (K/16)(\delta c_0)^2, \quad \delta L_c = 4(\sqrt{K_1} + \sqrt{K_2})^2/\Delta \simeq 16/|\delta c_0|. \quad (7)$$

(The approximate expressions assume that the heterogeneity is mainly manifested in different  $c_0$  rather than different  $K$ .) The dimensions of the step are finite at the critical compression,  $h_c = \delta L_c \simeq 16/\delta c_0$ . Yet, the lateral compressibility diverges,  $\partial \delta L/\partial \gamma \sim (v_c - v)^{-1/2}$  as  $v \rightarrow v_c$ , implying instability; extra area can be pulled into the inflected region without resistance, and the monolayer tries to curl up. (Detailed description of this critical response, however, is beyond the scope of the current model.) Macroscopically, the instability should show up as a plateau in the pressure-area isotherm of the monolayer.

Substituting typical values for phospholipid monolayers [20] —  $\gamma \simeq 10\text{--}50$  erg/cm<sup>2</sup>,  $K \simeq 10\text{--}50$   $k_B T$ ,  $c_0^{-1} \simeq 5\text{--}10$  nm — we get  $\lambda \simeq 1\text{--}10$  nm,  $v \simeq 0.1\text{--}1$ , and  $h \simeq 0.1\text{--}10$  nm. Hence, the mesas are sharp but shallow. The numerical value of  $v \sim 1$  implies that the predicted instability may be encountered for attainable pressures. Furthermore, the energy per unit length gained by departing from a flat conformation is  $g \simeq \Delta \simeq 1\text{--}10$   $k_B T/\text{nm}$  (or a few

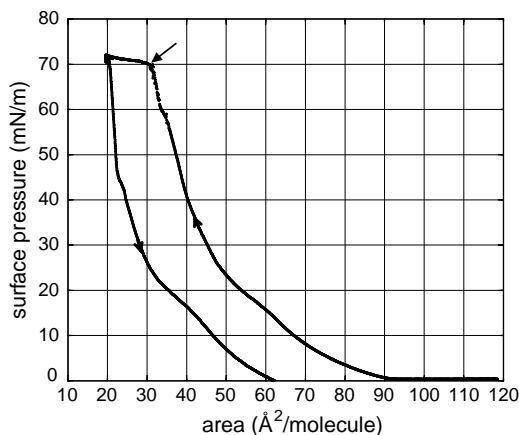


Fig. 2 – Pressure-area isotherm for a mixed monolayer of DPPC and POPG, as measured during a compression/expansion cycle in a Langmuir trough. The mole ratio is DPPC:POPG=7:3 and the temperature 25°C. The folding instability is indicated by an arrow.

piconewtons). Hence, for a typical domain size of about 1–10  $\mu\text{m}$ , the sigmoidal conformation is robust to thermal fluctuations<sup>(1)</sup>.

In recent experiments on model lung surfactant monolayers a new type of instability has been observed [18]. As the monolayer is compressed into the coexistence region, containing domains of different composition, there is a critical lateral pressure at which it locally folds towards the aqueous phase. Similar folding has been observed in simpler phospholipid mixtures as well [18]. Figure 2 shows a pressure-area isotherm as measured for a mixed monolayer of dipalmitoylphosphatidylcholine (DPPC) and palmitoyloleoylphosphatidylglycerol (POPG). The folding is manifested by a plateau in the isotherm, occurring, for this system, at a very low surface tension. (The same phenomenon, however, was observed in DPPG monolayers at a much higher surface tension [18].) Figure 3 presents a sequence of fluorescence microscopy snapshots of the monolayer just before and just after the instability. A micron-scale fold appears in between domain walls, subsequently propagating to nearby domains. The folding, as compared to other collapse mechanisms, significantly reduces irreversibility and loss of surfactant during a compression/expansion cycle. It is believed, therefore, to be of importance for the function of lungs. We suggest that the observed folding might be initiated by the conformation instability as found from the model. According to the model, the folding should follow the domain boundary, unlike the straight fold in fig. 3. Nevertheless, the surface shear viscosity of such monolayers is of order 1 surface poise ( $\text{dyn s/cm}$ ) [21]. For surface pressures smaller than  $10^2$   $\text{dyn/cm}$  this suggests a shear relaxation time larger than  $10^{-2}$  s. Since the fold forms on a time scale of about  $10^{-2}$  s (see fig. 3), the monolayer may respond to the instability like an elastic sheet, thus inhibiting curved folds. Certainly, more experiments are required before a clear relation between the observed folding and theoretical instability can be established.

In summary, we find that a Langmuir monolayer should exhibit inflected profiles in the vicinity of domain boundaries. These profiles are the elastic response to the contrast in

<sup>(1)</sup>One might worry about the gravitational energy cost of displacing water from the flat interface. This energy per unit area is about  $\delta\rho gh^2 \sim 10^4 k_B T/\text{cm}^2$ , where  $\delta\rho$  is the difference in density of the two phases and  $g$  the gravitational acceleration. Thus, due to the small height differences, gravity is negligible over all relevant lateral length scales (up to meters). Beyond the instability, however, the monolayer may become much more folded, and gravity may have a significant stabilizing role.

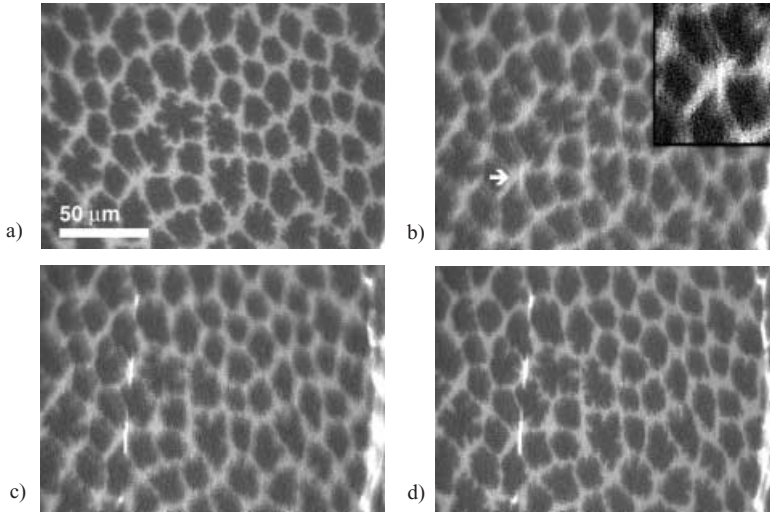


Fig. 3 – Fluorescence microscopy images of the folding instability. a) Section of the monolayer just before folding ( $t = 0$ ), exhibiting the biphasic domain structure. Dark regions are DPPC-rich; bright ones are PPG-rich. b) The same section at  $t = 1/30$  s. A micron-scale fold appears in between domain walls (indicated by arrow). The image is blurred because of monolayer movement during folding. The inset shows a contrast-enhanced image of the fold, magnified by 50 percent. c) The fold at  $t = 2/30$  s, having propagated to nearby domains. d) The fold at  $t = 4/30$  s, after the fast monolayer movement has ceased.

spontaneous curvature and/or bending rigidity between the two domains. For a monolayer composed of many coexisting domains, this leads to an overall conformation of “mesas”, where the domains of higher  $Kc_0$  stick down towards the aqueous phase. As the monolayer is compressed, the mesas grow more pronounced, subsequently developing small overhangs at their edges, and finally becoming unstable. Within the current model we could obtain the folding point only from an instability criterion. In practice, the folded structure may become favorable before the instability (*i.e.*, for  $\theta_0 < \pi$ ), whereupon folded regions would coexist with unfolded ones. (In addition, the shape instability might be pre-empted by other collapse mechanisms, as mentioned in the introduction.)

Apart from the folding instability, two rather general conclusions arise from this analysis. First, a biphasic Langmuir monolayer at a water-air or water-oil interface should practically never be completely flat; a conformation of mesas should appear for any finite surface tension. Such mesas are expected to exist, therefore, in many experimental and natural systems. Conversely, monolayers at water-oil interfaces in emulsions, microemulsions or  $L_3$  phases [20], whose surface tension practically vanishes, cannot have contiguous regions of differing elastic properties. At a vanishing tension any such heterogeneity would necessarily yield a shape instability. Indeed, to the best of our knowledge, no microdomain structures have ever been observed in those systems, as opposed to Langmuir monolayers.

Several issues remain to be examined. One is the stability of a straight domain boundary (*i.e.*, possible rippling of the mesa wall). Another is the effect of introducing a domain boundary of finite thickness. These issues will be addressed in a forthcoming publication [15]. Finally, it should be noted that the theoretical findings presented here do not conform with the conventional picture of *flat* lipid monolayers below the buckling transition. Since the model relies on very few, plausible assumptions, we believe that the inferred conformation of mesas

should be observed in practice. Such an observation, however, may be difficult in view of the small height differences involved, and the fluid interface on which the monolayer is deposited. We hope that this work will motivate experiments in this new, intriguing direction.

\* \* \*

We benefited from discussions and correspondence with D. ANDELMAN, J. KLEIN and S. SAFRAN. This work was supported by the National Science Foundation under Awards Nos. DMR 9975533 and 9728858, and by its MRSEC program under Award No. 9808595. HD was partially supported by the American Lung Association (RG-085-N). AG was supported by the Searle Scholars Program/The Chicago Community Trust (99-C-105). The experimental apparatus was made possible by an NSF CRIF/Junior Faculty Grant (CHE-9816513). KYCL is grateful for support from the March of Dimes Basil O'Connor Starter Scholar Research Award (5-FY98-0728), and the David and Lucile Packard Foundation (99-1465).

## REFERENCES

- [1] LANGEVIN D. and MEUNIER J., *Micelles, Membranes, Microemulsions, and Monolayers*, edited by W. M. GELBART, A. BEN-SHAUL and D. ROUX (Springer-Verlag, New York) 1989.
- [2] BIRDY K. S., *Lipid and Biopolymer Monolayers at Liquid Interfaces* (Plenum Press, New York) 1989.
- [3] ROBERTSON B. and HALLIDAY H. L., *Biochim. Biophys. Acta*, **1408** (1998) 346.
- [4] MILNER S. T., JOANNY J.-F. and PINCUS P., *Europhys. Lett.*, **9** (1989) 495.
- [5] SAINT-JALMES A., GRANER F., GALLET F. and HOUCHEMANDZADEH B., *Europhys. Lett.*, **28** (1994) 565.
- [6] HU J.-G. and GRANEK R., *J. Phys. II*, **6** (1996) 999.
- [7] ANDELMAN D., BROCHARD F. and JOANNY J.-F., *Proc. Natl. Acad. Sci. USA*, **84** (1987) 4717.
- [8] LEIBLER S. and ANDELMAN D., *J. Phys. (Paris)*, **48** (1987) 2013.
- [9] ANDELMAN D., KAWAKATSU T. and KAWASAKI K., *Europhys. Lett.*, **19** (1992) 57; KAWAKATSU T., ANDELMAN D., KAWASAKI K. and TANIGUCHI T., *J. Phys. II*, **3** (1993) 971; TANIGUCHI T., KAWASAKI K., ANDELMAN D. and KAWAKATSU T., *J. Phys. II*, **4** (1994) 1333.
- [10] WANG Z. G., *J. Chem. Phys.*, **99** (1993) 4191.
- [11] KODAMA H. and KOMURA S., *J. Phys. II*, **3** (1993) 1305.
- [12] MACKINTOSH F. C. and SAFRAN S. A., *Phys. Rev. E*, **47** (1993) 1180.
- [13] JÜLICHER F. and LIPOWSKY R., *Phys. Rev. E*, **53** (1996) 2670; SUNIL KUMAR P. B. and RAO M., *Phys. Rev. Lett.*, **80** (1998) 2489; GÓZDZ W. T. and GOMPPER G., *Phys. Rev. E*, **59** (1999) 4305; SUNIL KUMAR P. B., GOMPPER G. and LIPOWSKY R., *Phys. Rev. E*, **60** (1999) 4610.
- [14] GUTTMAN G. D. and ANDELMAN D., *J. Phys. II*, **3** (1993) 1411.
- [15] DIAMANT H., WITTEN T. A. and LEE K. Y. C., in preparation.
- [16] RIES H. E. and SWIFT H., *Langmuir*, **3** (1987) 853.
- [17] TCHORELOFF P., GULIK A., DENIZOT B., PROUST J. E. and PUISIEUX F., *Chem. Phys. Lipids*, **59** (1991) 151.
- [18] LIPP M. M., LEE K. Y. C., ZASADZINSKI J. A. and WARING A. J., *Science*, **273** (1996) 1196; LIPP M. M., LEE K. Y. C., WARING A. and ZASADZINSKI J. A., *Biophys. J.*, **72** (1997) 2783; LIPP M. M., LEE K. Y. C., TAKAMOTO D. Y., ZASADZINSKI J. A. and WARING A. J., *Phys. Rev. Lett.*, **81** (1998) 1650.
- [19] HARDEN J. L. and MACKINTOSH F. C., *Europhys. Lett.*, **28** (1994) 495.
- [20] SAFRAN S. A., *Statistical Thermodynamics of Surfaces, Interfaces, and Membranes* (Addison-Wesley, New York) 1994.
- [21] MILLER R., WÜSTNECK R., KRÄGEL J. and KRETZSCHMAR G., *Colloid Surf. A*, **111** (1996) 75; KRÄGEL J., KRETZSCHMAR G., LI J. B., LOGLIO G., MILLER R. and MÖHWALD H., *Thin Solid Films*, **285** (1996) 361.